International Journal of Applied Science and Engineering

Preliminary study on defect detection for sandwich composites using Impact-Echo method

Ying-Tzu Ke[1], Yung-Chiang Lin[1*], Chia-Chi Cheng[1], Jien-Chen Chen[2], Yu-Hung Pai[2], Keng-Tsang Hsu[1]

[1] *Department of Civil and Construction Engineering, Chaoyang University of Technology, Taichung City 413310, Taiwan, R.O.C.*
[2] *Industrial Technology Research Institute, Chutung, Hsinchu 31057, Taiwan, R.O.C.*

ABSTRACT

The sandwich composites in this study are laminated structures with two outer thin glass fiber reinforced panels and one or more thick lightweight foam panels as the core material. Such sandwich composites are often used in wind turbine blade. The Impact-Echo method using a microphone as a receiver was used to test the sandwich composite panel specimens. The signals were analysed in the frequency domain and normalized by the Rayleigh wave amplitude. Preliminary results show that thicker plates generally have a lower maximum peak frequency (MPF) for specimens without defects, but MPFs are more unstable due to the higher number of layers of the inner foam plate. Internal defects generated by excavating the core material, with lateral dimensions as small as 20 mm, can be identified from lower MPF and higher maximum peak amplitude in the normalized amplitude spectrum.

Keywords: Impact-Echo, Sandwich composites, Normalized amplitude spectrum, Wind turbine blades, Defect.

OPEN ACCESS

Received: November 22, 2022
Revised: January 3, 2023
Accepted: January 16, 2023

Corresponding Author:
Yung-Chiang Lin
yclin1977@cyut.edu.tw

Publisher:
Chaoyang University of Technology
ISSN: 1727-2394 (Print)
ISSN: 1727-7841 (Online)

1. INTRODUCTION

Wind power is an important green energy source. The west coast and the Taiwan Strait have excellent wind farms. With the strong support of the government, many wind turbine facilities have been installed around the island of Taiwan, and related research has been continuously proposed as provide by Wang et al. (2022).

A large number of sandwich composite materials are used on wind turbine blades and other parts to reduce weight and maintain adequate mechanical properties. The sandwich composites are usually referring to laminated structures with two outer thin glass fiber reinforced panels and one or more thick lightweight foam panels as the core material. How to effectively detect defects in the composite material is a very important issue for the maintenance and factory quality control of wind turbine blades. Numerous non-destructive methods, such as infrared thermal imaging and ultrasonic methods, are used for quality assurance and maintenance of wind turbine components. Many of these non-destructive inspection methods are used for blade defect or weld bead quality inspection (Juengert et al., 2009). For example, Amenabar et al. (2011) performed NDT on wind turbine blades with delaminated defects using ultrasonic, shearography, thermography and X-ray CT techniques. Amenabar (2017) inspected wind turbine blades with accessible advanced ultrasonic phased array technology. They both succeed to obtain reliable and clearly results on fan blades placed on the ground. However, with the exception of thermography, none of these methods can be easily applied to the operating wind turbine blades on-site.

A mature stress wave method, the impact-echo method (IE) has the advantages of broad frequency bandwidth and point contact with no need of coupling gel comparing with the ultrasonic method (Sansalone et al., 1997). Therefore, this method

has the potential to apply on the wind turbine blade. Amiri et al. (2017) used finite-element method to simulate the impact-echo method applied on glass fiber boards with a thickness of 6 to 12 mm. For a ratio of impactor-receiver distance to plate thickness of 0.3, numerical simulations show the main peak frequency corresponding to the plate thickness. Juengert and Grosse (2009) investigated full-scale wind turbine blades using ultrasound and sound waves. The sound waves were generated by the impulse hammer and the signals were recorded by a microphone. The contact time of the impluse hammer was reportedly longer at the area with the glass fiber-foam sandwich composite and and shorter at the area with only fiberglass plate. The debonded area was detected by the longer contact duration. In this study, we performed the IE tests on the fiberglass-foam sandwich composite panels of different thicknesses and the composite panels containing internal defects of different lateral dimensions using a small steel ball as the impactor and a microphone as a receiver. The amplitude spectra of the signal recorded by the microphone were analysed.

2. RESEARCH METHODS

In this study, the IE impactor was a small steel ball, and the receiver was a non-contact microphone placed right next to the impactor, 4 mm from the surface. The recording waveform was normalized by the amplitude of the Rayleigh wave response in the amplitude spectrum (Cheng et al., 2007). The basic idea of the method is as follow. When a test performed directly above an internal defect, the introduced impact energy generated a flexural vibration of the section above the defect. Compared to the intact plate, it obtains a larger amplitude response corresponding flexural modal frequency. However, the amplitude corresponding to the defected and intact panel cannot be compared since the amplitude in the frequency domain would be affected by the impacting magnitude and the impact-force are varied for different tests. In previous studies, the IE response was normalized by the vertical displacement of R-wave because the maximum vertical displacement of the R-wave recorded by the displacement receiver is proportional to the magnitude of the impact force for the impactor having the same impact-duration and with the same impactor-receiver distance in an isotropic media. The receiving R-wave waveform can be used as the simulated force-time function (Yu et al., 2006).

For this case, the mechanical waves generated by the steel ball hitting the surface of the composite plate are transmitted through the air and recorded by a microphone. The vertical component of the R-wave is easier to record because it is more likely to produce sound pressure changes in the air. Therefore, the R-wave signal received by the microphone is similar to the R-wave recorded by the displacement receiver. Since the impact-duration was similar for multiple tests on smooth surfaces, and for small impactor-receiver distances, the dispersion of the R-wave corresponding to the laminated composite is negligible, the normalized IE response can be determined by using the microphone's R-wave response as a simulated force-time function. The normalized IE spectrum is calculated as the ratio of the amplitude spectrum obtained from the waveform recorded by the microphone to the amplitude spectrum of the R-wave signal separated from the waveform.

The steady peak amplitude for repetitive tests on the same position after normalization is demonstrated in Fig.1. Due to the different magnitude of the tapping force, the peak amplitudes are 54.23, 67.05, 76.68 for the three repetitive tests, as shown in Fig 1(a). In contrast, the corresponding normalized peak amplitudes are 14.11, 15.47, and 14.05, as shown in Fig. 1(b). Thus, both peak amplitude and frequency can be the parameters for defect detection after normalization.

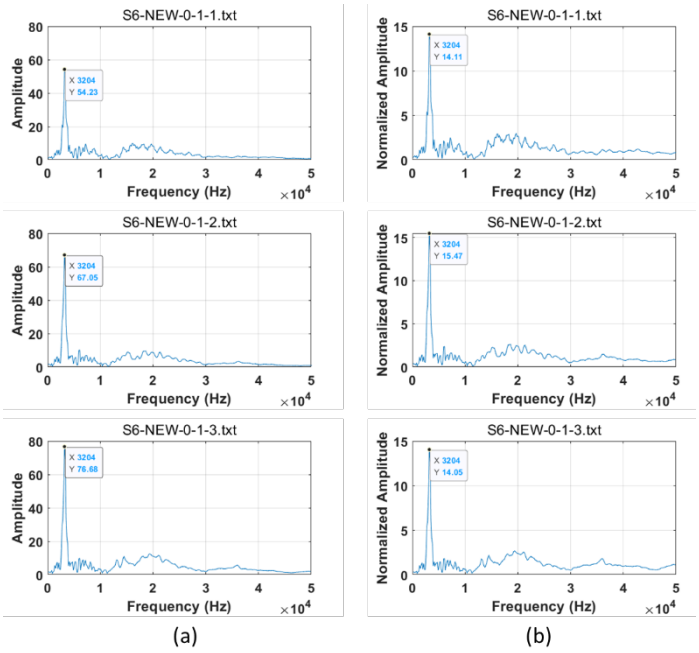

Fig. 1. The frequency response of different time measurements at same position: (a) results without normalized, (b) Normalized results

2.1 The Equipment and Setup

In IE method, the instrument consists of a small steel ball and a microphone receiver, as shown in Fig. 2. In this study, we used 3 mm steel balls as the impact source and a PCB microphone, which is modelled as PCB378C01 and has a frequency range of 4 to100000 Hz at +2 to -3 dB, as the receiver. The data acquisition card, Pico Scope 4224, has two channels with a maximum recording rate of 20 MHz, a voltage resolution of 12 bits, and a voltage range of ± 10 mv to ± 20 V. For each test, the total data points are 8192 points and the sampling time interval is 0.8 μs, and the frequency resolution is about 150 Hz.

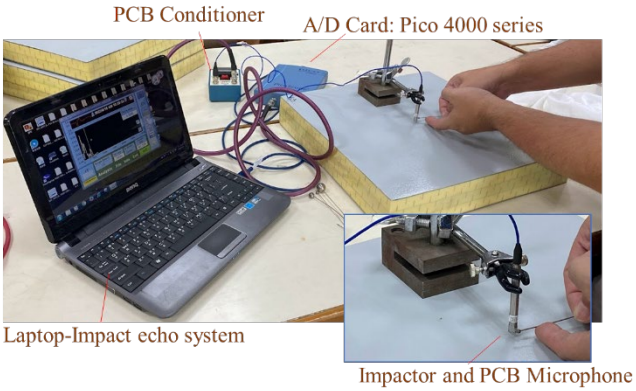

Fig. 2. Test equipment and application photos

2.2 The Experimental Specimens

The experimental specimens are 8 pieces of 40 by 40 cm plate specimens made by sandwich composite materials with different thicknesses and the defects with different lateral sizes, labelled by S1, S2-1, S2-2, S3, S4, S5, S6, and S7, as shown in Fig. 3. The sandwich structures are composed by the top and bottom fiberglass layer and the middle foaming layers glued by epoxy resin. The fiberglass parts contain 4 layers of fiberglass laminates placed 90 degrees in orientation to each other. The plate surfaces are covered by elastomeric paint. Three of the 4 cm thick specimens have defect. The defect, is located in the central of each specimen and the sizes are 2 by 2 cm, 5 by 5 cm, and 10 by 10 cm. Core material is removed in the defect area. The 2, 4 and 6 cm-thick plate contain 1, 2 and 3 layers of foaming panel, respectively.

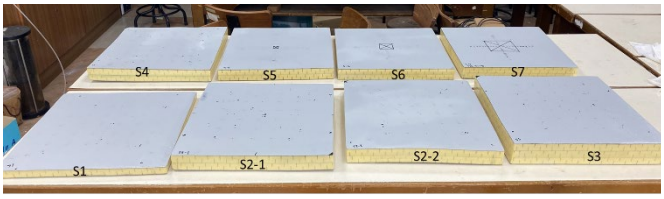

	Size	Defect
S1	40cm*40cm*2cm	0
S2-1, S2-2, S4	40cm*40cm*4cm	0
S3	40cm*40cm*6cm	0

	Size	Defect
S5	40cm*40cm*4cm	2cm*2cm
S6	40cm*40cm*4cm	5cm*5cm
S7	40cm*40cm*4cm	10cm*10cm

Fig. 3. The experimental specimens and their dimensions

3. RESULTS AND DISCUSSIONS

3.1. Test Results of Plate with Different Thicknesses

When impact-echo testing is performed on solid composite panels of different thicknesses, the thinner panels will have a stronger response with higher frequencies corresponding to the thickness of the panels. The multi-layered foaming material in between the fiberglass sheets results in more complex response. As illustrative examples, Fig 4 shows typical waveforms and spectral responses for the sandwich composite specimens with thicknesses of 2, 4, and 6 cm. As indicated in Fig. 4(a), for the case with a 2 cm-thick plate, the periodic responses shown in the waveform after the surface waves are very distinct with a period of about 0.000100 to 0.000105 s, which results in a peak frequency of about 9766 Hz in the normalized amplitude spectrum. When the thickness increases to 4 cm as shown in Fig. 4(b), the main period of the waveform is about 0.000140 to 0.000160 s, and the peak frequency is 6561 Hz. For the case with the thickness of 6 cm shown in Fig. 4(c), the main period of the waveform is 0.000170 to 0.000210 s, and the peak frequency is 5188 Hz in the amplitude spectrum. The response in the spectrum is more complex as the thickness becomes larger. The normalized peak amplitudes corresponding to 2, 4 and 6 cm thicknesses are 7.54, 4.971 and 3.107, respectively, indicating the less pronounced response for thicker plates. In the following sections, the maximum amplitude peak frequency and the corresponding normalized maximum amplitude are denoted as MAPF and NMA, respectively.

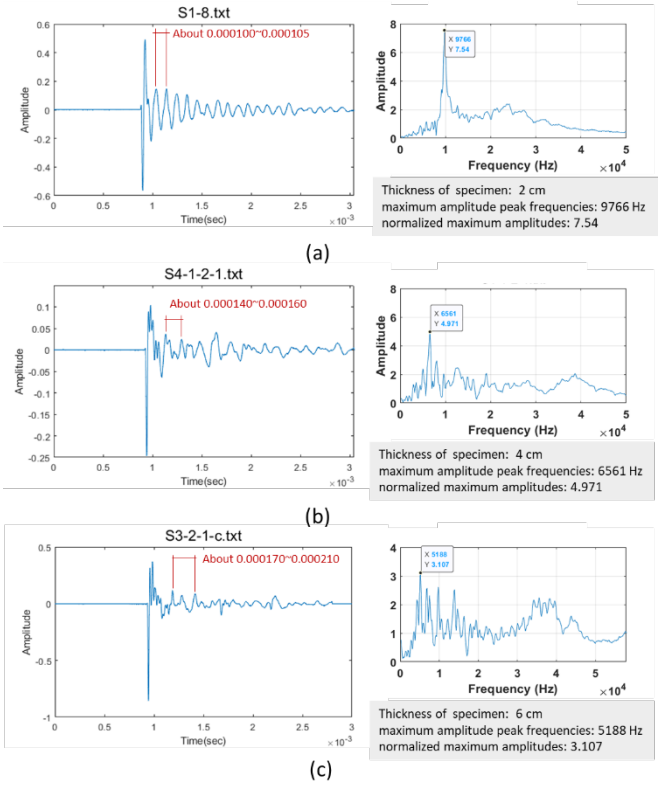

Fig. 4. The typical results of different thickness specimens: (a) 2 cm, (b) 4 cm and (c) 6 cm

Figs. 5-8 demonstrate the MAPF and NMA for tests performed on thirty points evenly spaced with 5 cm in intervals with labelling 1 to 30. The test results for S1 specimen are shown in Fig. 5. The results on the left of Fig. 5(a) indicate the MAPF and on the right show the corresponding NMA. The distribution of MAPFs are stably around 9000 to 1000 Hz and the NMAs are mostly around 4 to 8. Fig. 5(b) shows the average values and S.D.s of MAPF and NMA for three repetitive tests on each test point.

Only the test point S4-11 has a fairly high amplitude, about 15, but the frequency is similar to the rest of the points.

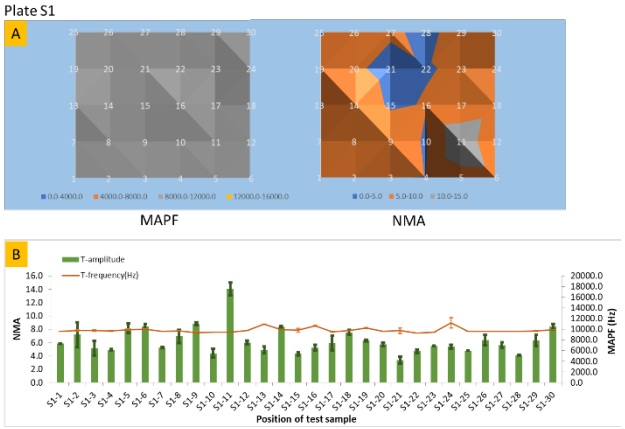

Fig. 5. The experimental results of specimen S1 with 2 cm thickness: (a) distribution of MAPF and NMA, (b) the distribution of the average values and S.D.s of MAPF and NMA for three repetitive tests

The specimens S2-2 and S4 with 4 cm thickness contain the core materials of two layers of foam panels. The distribution of MAPF and NMA are shown in Figs. 4 and 5 for S2-2 and S4, respectively. In Fig. 6(a), the MAPF of the S2 specimen is distributed between 6000 and 8000 Hz. Some measurement points where the MAPF reaches 10000-14000 Hz, shown in grey and yellow in the left of Fig. 6(a), may be caused by poor adhesion between the first and second foam layers. The NMA is mostly distributed between 2 and 4. S2-2-11, S2-2-21, and S2-2-28 have a slightly higher amplitude. As shown in Fig. 6(b), the maximum amplitude is at S2-2-21 with NMA equal to 6.4. Some of the point with large S.D. in MAPF indicates the maximum amplitude peak is jumping between the group around 6000 and 10000 Hz. The NMA is rather consistent for 3 repetitive tests

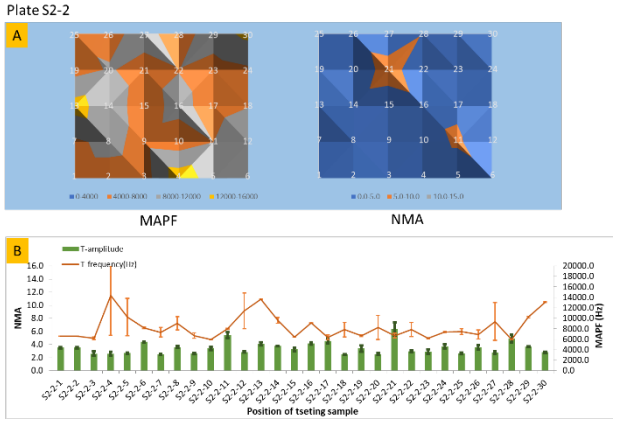

Fig. 6. The experimental results of specimen S2-2 with 4 cm thickness: (a) distribution of MAPF and NMA, (b) the distribution of the average values and S.D.s of MAPF and NMA for three repetitive tests

As shown in Fig. 7(a), the MAPF of the S4 specimen are mostly distributed around 6000-8000 Hz. Some peak frequencies reaching 12000-16000 Hz are distributed at the edge of the specimen, which may be caused by the poor bonding in the foam layers. Similar to specimen S2-2, the peak amplitude is mostly around 3 to 6. The location at S4-18 may have a defect right below the top layer because of its higher NMA value, 9.4, and a relatively lower MPAF, 2543 Hz.

Fig. 8 shows the results of the S3 specimen containing three foam layers, with a thickness of 6 cm. As shown in Fig. 8(a), the normal MPAF is about 6000 Hz, and the NMA is between 2 to 5. MPAFs are more unstable than ones obtained from the plate with thicknesses of 2 and 4 cm. As shown in Fig. 8(b), the S.D.s of MPAF are significant for some test points, indicating that MPAF varies considerably for different strikes. The most likely defective location is S3-11, which has a low MPAF of about 3204 Hz and a high NMA of about 6.5.

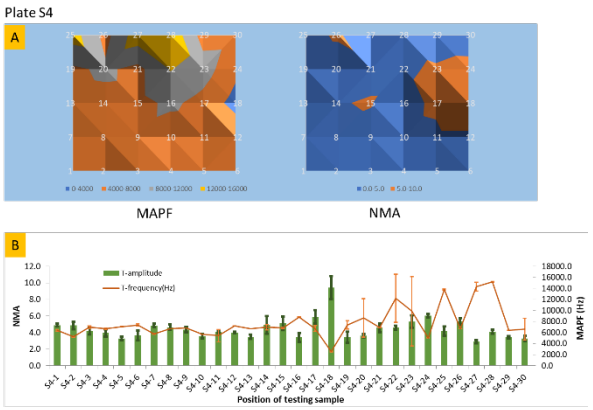

Fig. 7. The experimental results of specimen S4 with 4 cm thickness: (a) distribution of MAPF and NMA, (b) the distribution of the average values and S.D.s of MAPF and NMA for three repetitive tests

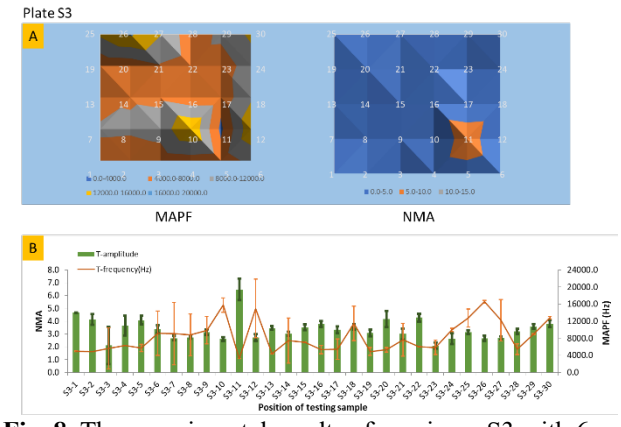

Fig. 8. The experimental results of specimen S3 with 6 cm thickness: (a) distribution of MAPF and NMA, (b) the distribution of the average values and S.D.s of MAPF and NMA for three repetitive tests

3.2 The Results for The Specimens with A Defect

For testing above the defective area, the time-domain waveforms received in defective areas have stronger and longer periodic responses than those in non-defective areas. Take the results of the S6 specimens with a defect area of 5 × 5 cm as an example, Fig. 9 shows the waveforms from microphone in position 0, 1, 2, 3, 4, 7, 8 cm from specimen centre. When the test position is located at the centre of the defect, position 0, the strong periodical response after the first high-frequency oscillation corresponds to the flexural mode of the upper fiberglass plate. When the test position moves away from the defect central, the periodic wave amplitude becomes smaller, and more high-frequency responses are generated. Fig. 10 shows the normalized amplitude spectra at positions 0 to 8. The peak frequency at the centre of the defect is about 3200 Hz. The peak frequency becomes 5188 Hz near the edge of the defect and moves to about 7000 Hz for tests away from the defective area. Besides, the high-frequency response at about 14000 Hz was found at the positions away from the defect due to the influence of the multi-layer composite structure. Fig. 10 also shows the normalized peak amplitude becomes more prominent for the test position near the centre of the defect.

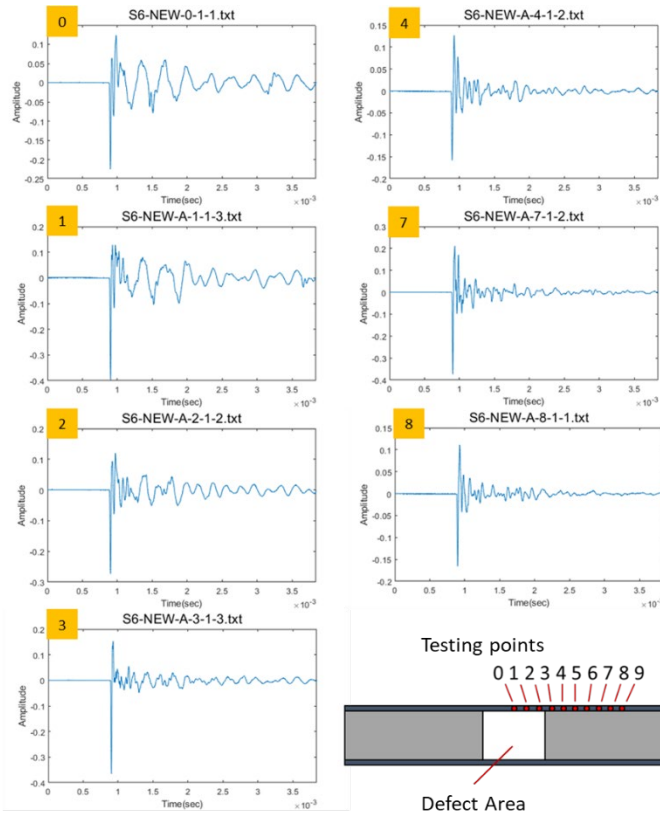

Fig. 9. The waveforms from microphone of specimen S6 in position 0, 1, 2, 3, 4, 7, 8 cm from specimen central

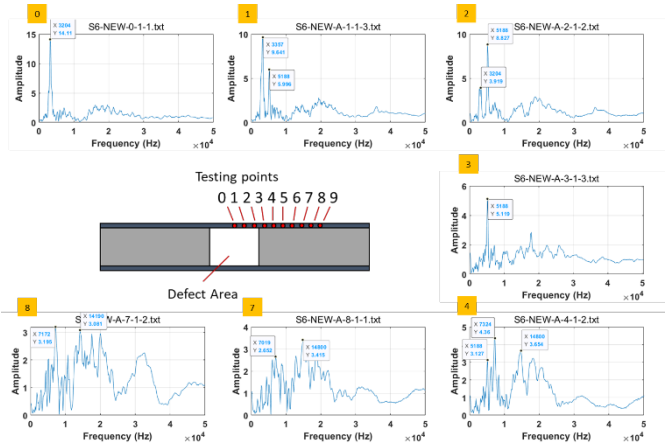

Fig. 10. The normalized frequency spectrums of specimen S6 in position 0, 1, 2, 3, 4, 7, 8 cm from specimen central

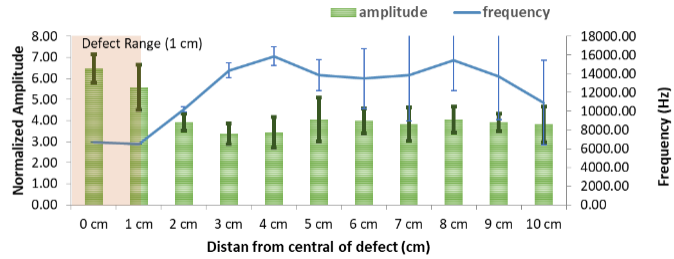

Fig. 9. The experimental results of specimen S5 with 4 cm thickness and 2 cm defect

S6 is a specimen containing a defect with a lateral size of 5 cm. The result shows in Fig. 10. In the defect area, 0, 1, and 2 cm, the MAPFs are about 3000~6000 Hz. They also have higher NMAs, about 8 to 12. When the receiver positions leave the defect area, the rise from 7000 Hz to 8000 Hz~12000 Hz, and the NMAs decreases to about 3 to 4. Some positions show significant variation for MAPF compared to the defect area with almost no variation.

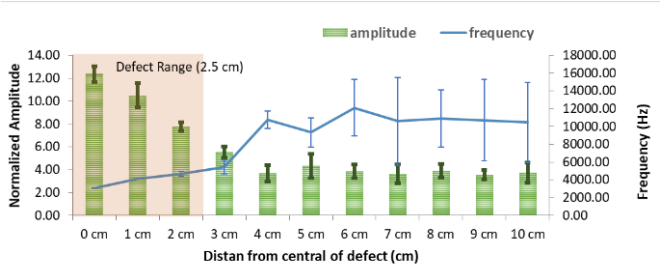

Fig. 8. The experimental results of specimen S6 with 4 cm thickness and 5 cm defect

S7 is a specimen containing a defect with a lateral size of 10 cm. The result shows in Fig. 11. At the defect position, 0 to 5 cm, the MAPFs are less than 1000 Hz at about 0-3 cm in the centre position, and the NMAs at 0-2 cm are above 5. For the receiver positions 3-5 cm from the centre of the

specimen, the MAPFs increase from 1000 to 7000 Hz. When the receiver positions leave the defect area, the average MAPFs are in the range between 8000 and 12000 Hz. The NMA decreases to 3-4 starting from 3 cm from the centre and beyond.

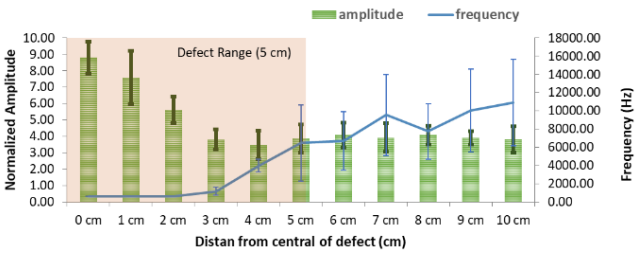

Fig. 11. The experimental results of specimen S7 with 4 cm thickness and 10 cm defect

4. CONCLUSIONS AND DISCUSSIONS

The sandwich specimens were glued layer by layer without vacuum the air to increase the interfacial bounding. As a result, for the solid panel, the MAPF is very consistent for the panel with one foam plate inside. However, for specimens with more foam board layers, the variation of MAPF at different positions or for the repeated tests will increase. Scatter test locations in the solid panel showed low MAPF and high NMA. These locations may have localized debonding between the top fiberglass layer and the foam layer, as the results were very similar to the ones at the prefabricated defective area.

For three panels containing defects of different sizes, the results showed low MAPF, high NMA and very small standard deviations (S.D.) for testing on the defective area. Furthermore, in testing near the center of the large defect, the MAPF is very low, which corresponds to the fundamental flexural mode of the top glass-fiber reinforced sheet. As the test approaches the edge of the large defect area, the MAPF gradually increases and the NMA gradually decreases, but the S.D. remains low.

The test results demonstrated that the primary peak frequency for the sandwich composite structures is lower for a thicker panel. For actual wind turbine blades, the thickness of the sandwich composite may vary from location to location. In the case of unknown thickness, multi-point detections are required to find abnormal signals due to interlayer delaminations. For defects just below the fiberglass layer, the location of the delamination can be easily identified by the low MAPF and high NMA in the normalized amplitude spectrum, regardless of the original thickness of the blade.

Comparing to the reviewed literatures (Juengert and Grosse, 2009; Amiri et al., 2017) this improved impact-echo technique not only requires no contact with the blade surface, but also does not require the use of a hammer to record the duration of the impact to obtain the contact time. It can be more easily used to detect delamination or assess the repair quality of wind turbine blades than using traditional displacement or ultrasonic transducers.

REFERENCES

Amenabar, I., Mendikute, A., López-Arraiza, A., Lizaranzu, M., Aurrekoetxea, J. 2011. Comparison and analysis of non-destructive testing techniques suitable for delamination inspection in wind turbine blades. Composites: Part B, 42, 1298–1305.

Amiri M. Tabatabaee Ghomi M. Non-destructive evaluation of glass-epoxy composite using Impact-Echo method. 2017. International Journal of Advanced Design and Manufacturing Technology, 10.

Juengert A., Grosse C. 2009. Inspection techniques for wind turbine blades using ultrasound and sound waves. Non-Destructive Testing in Civil Engineering (NDTCE'09), Nantes, France.

Lamarre, A. 2017. Improved inspection of composite wind turbine blades with accessible advanced ultrasonic phased array technology. 15th Asia Pacific Conference for Non-Destructive Testing (APCNDT2017), Singapore.

Cheng, C.C., Lin, Y., Hsiao, C.M., Chang, H.C. 2007. Evaluation of simulated transfer functions of concrete plate derived by impact-echo method. NDT & E International, 40, 239–249.

Juengert, A., Grosse, C.U. 2009. Inspection techniques for wind turbine blades using ultrasound and sound waves. Proceedings of 7th International Symposium on Nondestructive Testing in Civil Engineering. Nantes, France.

Sansalone, M.J., Streett, W.B., 1997. Impact-echo: Nondestructive evaluation of concrete and masonry. Bullbrier Press. Pennsylvania. USA.

Wang, W., Xue Y., He, C., Zhao, Y. 2022. Review of the typical damage and damage-detection methods of large wind turbine blades. Energies, 15, 5672.

Yu, C.P., Cheng, C.C., Lai, J. 2006. Application of closed-form solution for normal surface displacements on impacted half space: Quantification of impact-echo signals. International Journal of Applied Science and Engineering, 4, 127–150.